American Mineralogist, Volume 76, pages 246–256, 1991

The crystal structure of werdingite, $(Mg,Fe)_2Al_{12}(Al,Fe)_2Si_4(B,Al)_4O_{37}$, and its relationship to sillimanite, mullite, and grandidierite

MARGARET L. NIVEN
Department of Chemistry, University of Cape Town, Private Bag, Rondebosch 7700, South Africa
DAVID J. WATERS,* JOHN M. MOORE
Department of Geology, University of Cape Town, Private Bag, Rondebosch 7700, South Africa

ABSTRACT

Werdingite, $(Mg_{0.84},Fe_{0.16})_2Al_{12}(Al_{0.79}Fe_{0.21})_2Si_4B_2(B_{0.77}Al_{0.23})_2O_{37}$, is a borosilicate mineral newly recorded from Namaqualand, South Africa, which has a structure based on chains of AlO_6 octahedra parallel to **c**, cross-linked by Si_2O_7 groups, Al and Mg in five coordination, Al and Fe tetrahedra, and B triangles. It is triclinic $P\bar{1}$, with $a = 7.995(2)$, $b = 8.152(1)$, $c = 11.406(4)$ Å, $\alpha = 110.45(2)$, $\beta = 110.85(2)$, $\gamma = 84.66(2)°$, $V = 650.5(3)$ Å^3, $Z = 1$. The structure was solved by direct methods and refined to $R = 0.044$ for 3584 reflections ($I_{rel} > 2\sigma I_{rel}$) and 132 parameters. Although werdingite contains five-coordinated sites superficially similar to those in grandidierite and andalusite, the structure is best understood as being based on that of sillimanite, to which it is related by the overall substitution 2B + (Mg,Fe) = 2Si + Al + 1.5(O) with local atomic displacements resulting from the loss of nonchain O atoms. The werdingite structure provides an explanation for the mechanism of B incorporation in sillimanite, which follows the same overall substitution, and sheds light on the nature of other mullite-like borosilicate phases encountered in experimental studies of the system MgO-Al_2O_3-B_2O_3-SiO_2-H_2O.

INTRODUCTION

Werdingite is a borosilicate mineral recently described by Moore et al. (1990). It occurs in a high grade metamorphic rock associated with kornerupine, sillimanite, hercynite, grandidierite, and Fe-Ti oxides at Bok se Puts, (30°7′S, 18°27′E) in the granulite-facies region of the Namaqualand metamorphic complex, South Africa. Its powder diffraction pattern is similar to those of sillimanite, mullite, grandidierite, and related octahedral-chain aluminosilicates. Furthermore, synthesis experiments by Werding and Schreyer (1984) in the Al-rich part of the system MgO-Al_2O_3-B_2O_3-SiO_2-H_2O have produced one or more unknown mullite-like phases with essential B and Mg, and G. Werding (personal communication) has recently succeeded in synthesizing the Mg-end-member $Mg_2Al_{14}B_4Si_4O_{37}$ in the anhydrous system. To shed light on the structural relationships of high-*T* borosilicates, and on the possible nature of the B substitution recorded in some natural sillimanites (Grew and Hinthorne, 1983; Grew and Rossman, 1985), we have undertaken a structural study of natural werdingite from Namaqualand.

A clear, untwinned, inclusion-free fragment of werdingite was selected from a concentrate separated from the werdingite-bearing sillimanite-oxide rock, sample VP-4. In this sample werdingite occurs as millimeter-sized crystals, commonly of short prismatic habit, with scattered inclusions of sillimanite. Many crystals show simple twinning. Some are invaded by a grandidierite-spinel symplectite, and optical study shows that in many cases the **c** axes of werdingite and grandidierite approximately coincide. The mean composition of werdingite in this sample is given in Table 1.

EXPERIMENTAL DETAILS

The unit cell was established as triclinic by the oscillation and Weissenberg methods, using Cu*Kα* radiation ($\lambda = 1.5418$ Å). Accurate cell parameters were determined by a least-squares refinement of the setting angles of 24 reflections ($16 \leq \theta \leq 17°$) which were automatically located and centered on an Enraf-Nonius CAD4 diffractometer with graphite monochromated Mo*Kα* radiation ($\lambda = 0.7107$ Å). The intensities were measured with an ω-2θ scan mode $\Delta\omega = (1.35 + 0.35 \tan \theta)°$, an aperture width $(1.25 + 1.05 \tan \theta)$mm and a maximum recording time of 40 s. A total of 3724 unique reflections were measured out to $\theta = 30°$. The intensities of three reference reflections were monitored every hour, and orientation checked every hundred measured reflections. The data were processed for Lorentz and polarization factors and an empirical absorbtion correction (North et al., 1968) was applied. The observed and calculated structure factors are in Table 2.[1] Further experimental details of the crystal and data measurement are reported in Table 3.

* Present address: Department of Earth Sciences, University of Oxford, Parks Road, Oxford OX1 3PR, United Kingdom.

[1] A copy of Tables 2 and 7 may be ordered as Document AM-91-450 from the Business Office, Mineralogical Society of America, 1130 Seventeenth Street NW, Suite 330, Washington, DC 20036, U.S.A. Please remit $5.00 in advance for the microfiche.

0003–004X/91/0102–0246$02.00

TABLE 1. Mean composition of werdingite from analyses by Moore et al. (1990)

	Cations per formula unit of 37(O)
Si	4.018
Ti	0.008
Al	14.206
Fe^{3+}	0.180
Fe^{2+}	0.678
Mg	1.347
B	3.564
Total	24.000
O	37.000

Note: Fe^{3+} calculated assuming a total positive charge of 74.

SOLUTION AND REFINEMENT OF THE STRUCTURE

For the solution and refinement of the structure 3584 reflections with $I_{rel} > 2\sigma(I_{rel})$ were considered observed. The structure was initially solved in the noncentrosymmetric space group $P1$ using the direct-methods program SHELXS-86 (Sheldrick, 1987), which afforded the location of Fe/Mg, Al, and Si atoms. Refinement of the structure was carried out with SHELX76 (Sheldrick, 1978). Observation of parameter correlation and centers of symmetry indicated $P\bar{1}$ as the preferred space group, and successful refinement of the structure with isotropic temperature factors in this system has vindicated its choice. Complex neutral atom scattering factors were taken from Cromer and Mann (1968), with dispersion corrections from Cromer and Liberman (1970). Molecular parameters were calculated using PARST (Nardelli, 1983). All computations were carried out using a VAX computer.

The unit cell has $Z = 1$ and hence only half of the structure, i.e., $(Mg,Fe,Al)_2Al_6Si_2B(B,Al)O_{18.5}$, had to be located. We distinguished between Al, Mg, and Si atoms by considering the number of and distance to adjacent O atoms, and the shape of the polyhedron so described; Al has four (irregular tetrahedron), five (irregular trigonal bipyramid), or six (irregular octahedron) O atoms, whereas Si has four O atoms defining a nearly regular tetrahedron. The Mg polyhedron is an irregular trigonal bipyramid, but its mean bond length of 1.985 Å is distinctly longer than that of an adjacent Al trigonal bipyramid at 1.844 Å. For comparison, mean bond lengths for the Mg and Al chain-bridging trigonal bipyramidal sites in grandidierite are 2.042 and 1.838 Å, respectively (Stephenson and Moore, 1968).

Four Al atoms Al(5)1, Al(5)2, Al(6)2, and Al(6)5 were located in general positions. Four additional Al atoms Al(6)1, Al(6)3, Al(6)4, and Al(6)6 were located at centers of symmetry and assigned a site occupancy of 0.5. The two Si atoms were located in general positions and underwent well-behaved refinement.

Part of the Fe was assigned to a tetrahedral site Fe(4)1, which showed the highest electron density. Since local charge balance indicates that this site should be occupied dominantly by trivalent cations, it was modeled by invoking partial occupancy by Fe and Al. Occupancy factors were refined with total occupancy 1.0 for the site, giving final occupancy values of Fe 0.21, Al 0.79. The

TABLE 3. Crystal data, details of the data collection, and refinement parameters for werdingite

Formula	$(Mg_{0.84}Fe_{0.16})_2Al_{12}(Al_{0.79}Fe_{0.21})_2Si_4B_2(B_{0.77}Al_{0.23})_2O_{37}$
Molar mass (g mol^{-1})	1203.58
Space group	$P\bar{1}$
a (Å)	7.995(2)
b (Å)	8.152(1)
c (Å)	11.406(4)
α (°)	110.45(2)
β (°)	110.85(2)
γ (°)	84.66(2)
V (Å^3)	650.5(3)
D_m (diiodomethane/acetone) (g cm^{-3})	3.04
D_c (g cm^{-3}) (for $Z = 1$)	3.07
μ(Mo$K\alpha$) (cm^{-1})	13.33
Crystal dimensions (mm)	0.45 × 0.50 × 0.55
Instability of standard reflections (%)	1
Percent transmission (absorption correction) (max, min, average)	99.8, 87.6, 94.7
Number of unique reflections	3724
Number of parameters	132
Number of reflections with $I_{rel} > 2\sigma(I_{rel})$	3584
$R = \Sigma\|\|F_o\| - \|F_c\|\|/\Sigma\|F_o\|$	0.044

TABLE 4. Fractional atomic coordinates and isotropic temperature factors (Å^2 × 10^4) for werdingite

Atom	x	y	z	U_{iso}
Fe/Al(4)1*	0.6624(1)	0.1674(1)	0.0827(1)	73(3)
Al(6)1**	0	0	0	53(2)
Al(6)2	0.0068(1)	0.0020(1)	0.2564(1)	44(2)
Al(6)3**	0	0	½	40(2)
Al(6)4**	½	½	0	49(2)
Al(6)5	0.5046(1)	0.4952(1)	0.2506(1)	40(2)
Al(6)6**	½	½	½	36(2)
Al(5)1	0.1523(1)	0.3177(1)	0.7413(1)	41(2)
Al(5)2	0.2297(1)	0.6777(1)	0.3522(1)	42(2)
Fe/Mg(5)1†	0.1209(1)	0.3153(1)	0.2353(1)	49(3)
Si(4)1	0.6496(1)	0.1554(1)	0.3354(1)	41(2)
Si(4)2	0.3503(1)	0.8406(1)	0.1812(1)	40(2)
B(3)1	0.2256(5)	0.2706(5)	0.5019(3)	59(6)
B(3)2‡	0.2261(7)	0.2652(8)	−0.0048(4)	47(8)
Al(4)2‡	0.2705(6)	0.2105(6)	−0.0071(4)	2(14)
O(1)	0.0278(3)	0.5437(3)	0.2690(2)	93(4)
O(2)	0.1579(3)	0.2009(3)	−0.1471(2)	77(4)
O(3)	0.1615(3)	0.2037(3)	0.5752(2)	64(4)
O(4)	0.6175(3)	0.2732(3)	0.2379(2)	86(4)
O(5)	0.6241(3)	0.2768(3)	−0.0391(2)	88(4)
O(6)	0.6330(3)	0.2875(3)	0.4762(2)	63(4)
O(7)	0.6434(3)	0.5626(3)	0.1768(2)	58(4)
O(8)	0.6403(3)	0.6034(3)	−0.0627(2)	61(4)
O(9)	0.3613(3)	0.7080(3)	0.2620(2)	64(4)
O(10)	0.3523(3)	0.4482(3)	0.3258(2)	47(4)
O(11)	0.1524(3)	0.1984(3)	0.0637(2)	107(5)
O(12)	0.1015(3)	−0.1238(3)	0.3714(2)	78(4)
O(13)	0.1580(3)	0.2014(3)	0.3662(2)	81(4)
O(14)	0.1525(3)	−0.0762(3)	0.1468(2)	60(4)
O(15)	−0.1479(3)	0.0815(3)	0.3609(2)	54(4)
O(16)	−0.0985(3)	0.1245(3)	0.1342(2)	107(4)
O(17)	0.3497(3)	0.4052(3)	0.5655(2)	57(4)
O(18)	0.5042(3)	−0.0061(3)	0.2692(2)	106(4)
O(19A)§	0.5905(16)	−0.0503(14)	0.0107(10)	108(18)
O(19B)§	0.5167(22)	0.0003(28)	0.0050(18)	72(18)

* Site occupancy Fe 0.21, site occupancy Al 0.79.
** Site occupancy 0.5.
† Site occupancy Fe 0.16, site occupancy Mg 0.84.
‡ Site occupancy B 0.77, site occupancy Al 0.23.
§ Site occupancy 0.25.

TABLE 5. Bond lengths (Å), angles (°) and O···O distances (Å) of polyhedron edges for werdingite

Al-O octahedra

Al(6)1-O(11)	1.883	Al(6)3-O(12)	1.868
-O(16)	1.902	-O(15)	1.900
-O(14)	1.952	-O(3)	1.943
Mean	1.912	Mean	1.904
O(11)-Al(6)1-O(14)	90.3	O(3)-Al(6)3-O(12)	94.8
O(11)-Al(6)1-O(16)	86.7	O(3)-Al(6)3-O(15)	91.2
O(14)-Al(6)1-O(16)	79.5	O(12)-Al(6)3-O(15)	82.2
O(11)-Al(6)1-O(11)[a]	180	O(3)-Al(6)3-O(3)[b]	180
O(14)-Al(6)1-O(11)[a]	89.7	O(12)-Al(6)3-O(3)[b]	85.2
O(16)-Al(6)1-O(11)[a]	93.3	O(15)-Al(6)3-O(3)[b]	88.8
O(14)-Al(6)1-O(14)[a]	180	O(12)-Al(6)3-O(12)[b]	180
O(16)-Al(6)1-O(14)[a]	100.5	O(15)-Al(6)3-O(12)[b]	97.8
O(16)-Al(6)1-O(16)[a]	180	O(15)-Al(6)3-O(15)[b]	180
O(14)-O(16)	2.464*	O(12)-O(15)	2.478*
O(11)-O(16)	2.598	O(3)-O(12)[b]	2.581*
O(11)-O(14)[a]	2.704	O(3)-O(15)[b]	2.690
O(11)-O(14)	2.719	O(3)-O(15)	2.745
O(11)-O(16)[a]	2.753	O(3)-O(12)	2.805
O(14)-O(16)[a]	2.963	O(12)-O(15)[b]	2.838
Al(6)6-O(10)	1.832	Al(6)4-O(7)	1.840
-O(6)	1.934	-O(8)	1.910
-O(17)	1.953	-O(5)	1.976
Mean	1.906	Mean	1.909
O(6)-Al(6)6-O(10)	97.2	O(5)-Al(6)4-O(7)	90.1
O(6)-Al(6)6-O(17)	90.7	O(5)-Al(6)4-O(8)	91.6
O(10)-Al(6)6-O(17)	99.2	O(7)-Al(6)4-O(8)	99.2
O(6)-Al(6)6-O(6)[c]	180	O(5)-Al(6)4-O(5)[d]	180
O(10)-Al(6)6-O(6)[c]	82.8	O(7)-Al(6)4-O(5)[d]	89.9
O(17)-Al(6)6-O(6)[c]	89.3	O(8)-Al(6)4-O(5)[d]	88.4
O(10)-Al(6)6-O(10)[c]	180	O(7)-Al(6)4-O(7)[d]	180
O(17)-Al(6)6-O(10)[c]	80.8	O(8)-Al(6)4-O(7)[d]	80.8
O(17)-Al(6)6-O(17)[c]	180	O(8)-Al(6)4-O(8)[d]	180
O(10)-O(17)[c]	2.456*	O(7)-O(8)[d]	2.431*
O(6)[c]-O(10)	2.493*	O(5)-O(7)[d]	2.698
O(6)-O(17)[c]	2.732	O(5)-O(7)	2.703
O(6)-O(17)	2.765	O(5)-O(8)[d]	2.709
O(6)-O(10)	2.825	O(5)-O(8)	2.787
O(10)-O(17)	2.884	O(7)-O(8)	2.856
Al(6)2-O(12)	1.853	Al(6)5-O(7)	1.829
-O(13)	1.881	-O(10)	1.851
-O(16)	1.905	-O(17)[c]	1.914
-O(14)	1.915	-O(4)	1.928
-O(15)	1.932	-O(8)[d]	1.945
-O(2)[a]	1.954	-O(9)	1.979
Mean	1.907	Mean	1.908
O(12)-Al(6)2-O(13)	95.1	O(4)-Al(6)5-O(7)	93.1
O(12)-Al(6)2-O(15)	81.8	O(4)-Al(6)5-O(9)	172.7
O(12)-Al(6)2-O(2)[a]	84.7	O(4)-Al(6)5-O(10)	92.8
O(12)-Al(6)2-O(14)	100.1	O(4)-Al(6)5-O(8)[d]	88.8
O(12)-Al(6)2-O(16)	177.7	O(4)-Al(6)5-O(17)[c]	91.5
O(13)-Al(6)2-O(15)	89.8	O(7)-Al(6)5-O(9)	93.4
O(13)-Al(6)2-O(2)[a]	177.3	O(7)-Al(6)5-O(10)	174.2
O(13)-Al(6)2-O(14)	91.3	O(7)-Al(6)5-O(8)[d]	80.1
O(13)-Al(6)2-O(16)	87.2	O(7)-Al(6)5-O(17)[c]	98.7
O(15)-Al(6)2-O(2)[a]	87.5	O(9)-Al(6)5-O(10)	80.7
O(15)-Al(6)2-O(14)	177.8	O(9)-Al(6)5-O(8)[d]	89.0
O(15)-Al(6)2-O(16)	97.7	O(9)-Al(6)5-O(17)[c]	90.9
O(2)[a]-Al(6)2-O(14)	91.4	O(10)-Al(6)5-O(8)[d]	99.7
O(2)[a]-Al(6)2-O(16)	93.0	O(10)-Al(6)5-O(17)[c]	81.4
O(14)-Al(6)2-O(16)	80.3	O(8)[d]-Al(6)5-O(17)[c]	178.8
O(14)-O(16)	2.464*	O(7)-O(8)[d]	2.431*
O(12)-O(15)	2.478*	O(10)-O(17)[c]	2.456*
O(12)-O(2)[a]	2.566*	O(9)-O(10)	2.482*
O(13)-O(16)	2.611*	O(4)-O(8)[d]	2.709
O(15)-O(2)[a]	2.688	O(4)-O(7)	2.727
O(13)-O(15)	2.691	O(4)-O(10)	2.736
O(13)-O(14)	2.714	O(4)-O(17)[c]	2.751
O(12)-O(13)	2.755	O(8)[d]-O(9)	2.751
O(14)-O(2)[a]	2.770	O(7)-O(9)	2.774
O(16)-O(2)[a]	2.800	O(9)-O(17)[c]	2.775
O(12)-O(14)	2.890	O(7)-O(17)[c]	2.839
O(15)-O(16)	2.891	O(8)[d]-O(10)	2.902

Table 5—*Continued*

	Al-O trigonal bipyramids		
Al(5)1-O(1)^{i}	1.742	Al(5)2-O(1)	1.792
-O(7)^{c}	1.751	-O(9)	1.795
-O(3)	1.821	-O(6)^{c}	1.805
-O(2)^{e}	1.824	-O(12)^{f}	1.822
-O(12)^{b}	2.364	-O(10)	2.007
Mean	1.900	Mean	1.866
O(7)^{c}-Al(5)1-O(12)^{b}	172.7	O(10)-Al(5)2-O(12)^{f}	175.4
O(2)^{e}-Al(5)1-O(3)	121.9	O(1)-Al(5)2-O(9)	121.5
O(1)^{i}-Al(5)1-O(3)	109.5	O(1)-Al(5)2-O(6)^{c}	122.9
O(1)^{i}-Al(5)1-O(2)^{e}	109.2	O(9)-Al(5)2-O(6)^{c}	110.5
O(7)^{c}-Al(5)1-O(2)^{e}	102.4	O(10)-Al(5)2-O(1)	84.4
O(7)^{c}-Al(5)1-O(3)	102.0	O(10)-Al(5)2-O(9)	81.3
O(7)^{c}-Al(5)1-O(1)^{i}	111.1	O(10)-Al(5)2-O(6)^{c}	81.5
O(12)^{b}-Al(5)1-O(2)^{e}	74.3	O(12)^{f}-Al(5)2-O(1)	91.1
O(12)^{b}-Al(5)1-O(3)	74.9	O(12)^{f}-Al(5)2-O(9)	101.7
O(12)^{b}-Al(5)1-O(1)^{i}	76.2	O(12)^{f}-Al(5)2-O(6)^{c}	100.5
O(2)^{e}-O(12)^{b}	2.566*	O(9)-O(10)	2.482*
O(3)-O(12)^{b}	2.581*	O(6)^{c}-O(10)	2.493*
O(1)^{i}-O(12)^{b}	2.580	O(1)-O(10)	2.557
O(3)-O(7)^{c}	2.777	O(1)-O(12)^{f}	2.580
O(2)^{e}-O(7)^{c}	2.786	O(6)^{c}-O(12)^{f}	2.788
O(1)^{i}-O(7)^{c}	2.880	O(9)-O(12)^{f}	2.806
O(1)^{i}-O(2)^{e}	2.907	O(6)^{c}-O(9)	2.958
O(1)^{i}-O(3)	2.910	O(1)-O(9)	3.131
O(2)^{e}-O(3)	3.186	O(1)-O(6)^{c}	3.160
	Fe/Mg trigonal bipyramid		
Mg(5)1-O(1)	1.901	O(10)-Mg(5)1-O(16)	168.4
-O(13)	1.945	O(1)-Mg(5)1-O(11)	118.3
-O(11)	1.951	O(1)-Mg(5)1-O(13)	118.3
-O(10)	1.973	O(11)-Mg(5)1-O(13)	123.2
-O(16)	2.154	O(10)-Mg(5)1-O(1)	82.6
Mean	1.985	O(10)-Mg(5)1-O(11)	96.6
		O(10)-Mg(5)1-O(13)	95.5
		O(16)-Mg(5)1-O(1)	109.0
		O(16)-Mg(5)1-O(11)	78.3
		O(16)-Mg(5)1-O(13)	79.0
O(1)-O(10)	2.557*		
O(13)-O(16)	2.611*		
O(11)-O(16)	2.598		
O(10)-O(13)	2.901		
O(10)-O(11)	2.930		
O(1)-O(13)	3.301		
O(1)-O(16)	3.305		
O(1)-O(11)	3.306		
O(11)-O(13)	3.427		
	Al/Fe		
Al(4)1-O(19B)	1.648	O(4)-Al(4)1-O(5)	121.7
-O(19A)	1.729	O(4)-Al(4)1-O(16)^{g}	105.2
-O(19B)^{h}	1.819	O(5)-Al(4)1-O(16)^{g}	105.4
-O(5)	1.825	O(4)-Al(4)1-O(19B)	102.4
-O(4)	1.826	O(5)-Al(4)1-O(19B)	104.3
-O(16)^{g}	1.828	O(4)-Al(4)1-O(19A)	111.6
-O(19A)^{h}	2.062	O(16)^{g}-Al(4)1-O(19B)	118.9
Mean	1.820	O(5)-Al(4)1-O(19A)	113.2
		O(16)^{g}-Al(4)1-O(19A)	95.7
		O(4)-Al(4)1-O(19B)^{h}	100.1
		O(5)-Al(4)1-O(19B)^{h}	101.1
		O(16)^{g}-Al(4)1-O(19B)^{h}	125.0
		O(4)-Al(4)1-O(19A)^{h}	91.0
		O(5)-Al(4)1-O(19A)^{h}	92.1
		O(16)^{g}-Al(4)1-O(19A)^{h}	144.0
O(16)^{g}-O(19A)	2.638	O(5)-O(16)^{g}	2.907
O(4)-O(19B)	2.709	O(4)-O(19A)	2.941
O(5)-O(19B)	2.744	O(5)-O(19A)	2.967
O(4)-O(19A)^{h}	2.777	O(16)^{g}-O(19B)	2.996
O(4)-O(19B)^{h}	2.795	O(4)-O(5)	3.189
O(5)-O(19A)^{h}	2.804	O(16)^{g}-O(19B)^{h}	3.234
O(5)-O(19B)^{h}	2.815	O(16)^{g}-O(19A)^{h}	3.700
O(4)-O(16)^{g}	2.902		

Table 5—*Continued*

		Si-O tetrahedra	
Si(4)1-O(18)	1.619	Si(4)2-O(18)^f	1.617
-O(6)	1.635	-O(9)	1.627
-O(15)^g	1.635	-O(14)^f	1.631
-O(4)	1.650	-O(5)^d	1.643
Mean	1.635	Mean	1.630
O(4)-Si(4)1-O(6)	106.8	O(9)-Si(4)2-O(14)^f	109.9
O(4)-Si(4)1-O(15)^g	107.8	O(9)-Si(4)2-O(18)^f	109.8
O(4)-Si(4)1-O(18)	111.7	O(9)-Si(4)2-O(5)^d	107.2
O(6)-Si(4)1-O(15)^g	109.9	O(14)^f-Si(4)2-O(18)^f	110.6
O(6)-Si(4)1-O(18)	110.5	O(14)^f-Si(4)2-O(5)^d	107.7
O(15)^g-Si(4)1-O(18)	110.1	O(18)^f-Si(4)2-O(5)^d	111.6
O(4)-O(6)	2.638	O(5)^d-O(9)	2.631
O(4)-O(15)^g	2.654	O(5)^d-O(14)^f	2.643
O(15)^g-O(18)	2.667	O(9)-O(18)^f	2.653
O(6)-O(18)	2.673	O(9)-O(14)^f	2.668
O(6)-O(15)^g	2.676	O(14)^f-O(18)^f	2.670
O(4)-O(18)	2.705	O(5)-O(18)^f	2.695
		B-O triangles	
B(3)1-O(17)	1.360	B(3)2-O(8)^d	1.390
-O(13)	1.363	-O(11)	1.393
-O(3)	1.391	-O(2)	1.427
Mean	1.371	Mean	1.403
O(3)-B(3)1-O(13)	118.6	O(2)-B(3)2-O(11)	118.9
O(3)-B(3)1-O(17)	120.1	O(2)-B(3)2-O(8)^d	119.8
O(13)-B(3)1-O(17)	121.3	O(11)-B(3)2-O(8)^d	121.3
O(3)-O(13)	2.367	O(8)^d-O(11)	2.425
O(13)-O(17)	2.374	O(2)-O(11)	2.427
O(3)-O(17)	2.383	O(2)-O(8)^d	2.436
		Al-O tetrahedron	
Al(4)2-O(11)	1.473	O(2)-Al(4)2-O(11)	109.1
-O(2)	1.506	O(2)-Al(4)2-O(8)^d	105.8
-O(8)^d	1.548	O(2)-Al(4)2-O(19A)^h	110.0
-O(19A)^h	1.633	O(8)^d-Al(4)2-O(11)	106.8
Mean	1.540	O(8)^d-Al(4)2-O(19A)^h	115.1
		O(11)-Al(4)2-O(19A)^h	109.8
O(8)^d-O(11)	2.425	O(11)-O(19A)^h	2.542
O(2)-O(11)	2.427	O(2)-O(19A)^h	2.573
O(2)-O(8)^d	2.436	O(8)^d-O(19A)^h	2.684

Note: * values denote shared edges. Mean sigma for bond lengths: 0.003 Å; mean sigma for bond angles: 0.02°.
^{a} $-x, -y, -z$.
^{b} $-x, -y, -z + 1$.
^{c} $-x + 1, -y + 1, -z + 1$.
^{d} $-x + 1, -y + 1, -z$.
^{e} $x, y, z + 1$.
^{f} $x, y + 1, z$.
^{g} $x + 1, y, z$.
^{h} $-x + 1, -y, -z$.
^{i} $-x, -y + 1, -z + 1$.

remaining Fe was assigned to the Mg(5)1 site, where a coupled refinement of Mg and Fe gave the final occupancy values Fe 0.16, Mg 0.84. The refinement thus indicates a total Fe content of 0.74 atoms per formula unit, compared with 0.86 from the chemical analysis.

Eighteen unique O atoms were located and refined satisfactorily. The remaining half–O atom, required by the stoichiometry from analytical results, is believed to be distributed between two sites O19A and O19B, each modeled with occupancy 0.25.

One B atom was assigned uniquely to site B(3)1. The subsequent residual electron density was best modeled by again invoking disorder and partial site occupancy. The chemical analysis indicates a B content of less than four atoms per formula unit, and so 0.8B and 0.2Al were assigned and allowed coupled-occupancy refinement, with a total of 1.0 (B + Al), at the sites B(3)2 and Al(4)2, respectively. The final occupancy values were B 0.77, Al

Table 6. Summary of sites and occupancies

Site	Multiplicity	Occupancy
	Octahedral sites	
Al(6)1	1	Al 1.0
Al(6)2	2	Al 1.0
Al(6)3	1	Al 1.0
Al(6)4	1	Al 1.0
Al(6)5	2	Al 1.0
Al(6)6	1	Al 1.0
	Trigonal-bipyramidal sites	
Al(5)1	2	Al 1.0
Al(5)2	2	Al 1.0
Mg(5)1	2	Mg 0.76, Fe 0.16, Al 0.08
	Tetrahedral sites	
Si(4)1	2	Si 1.0
Si(4)2	2	Si 1.0
Fe(4)1	2	Fe 0.21, Al 0.79
Al(4)2	2	Al 0.23
	Planar triangular sites	
B(3)1	2	B 1.0
B(3)2	2	B 0.77

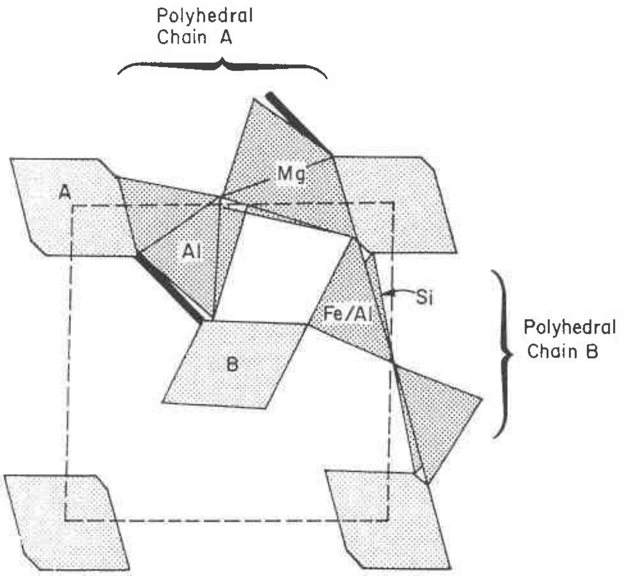

Fig. 1. Plan view of part of the werdingite unit cell, projected down [001], showing the arrangement of octahedral AlO_6 chains (dark shading) and double chains of bridging polyhedra (stippled). Vertical BO_3 triangles shown as dark solid bars.

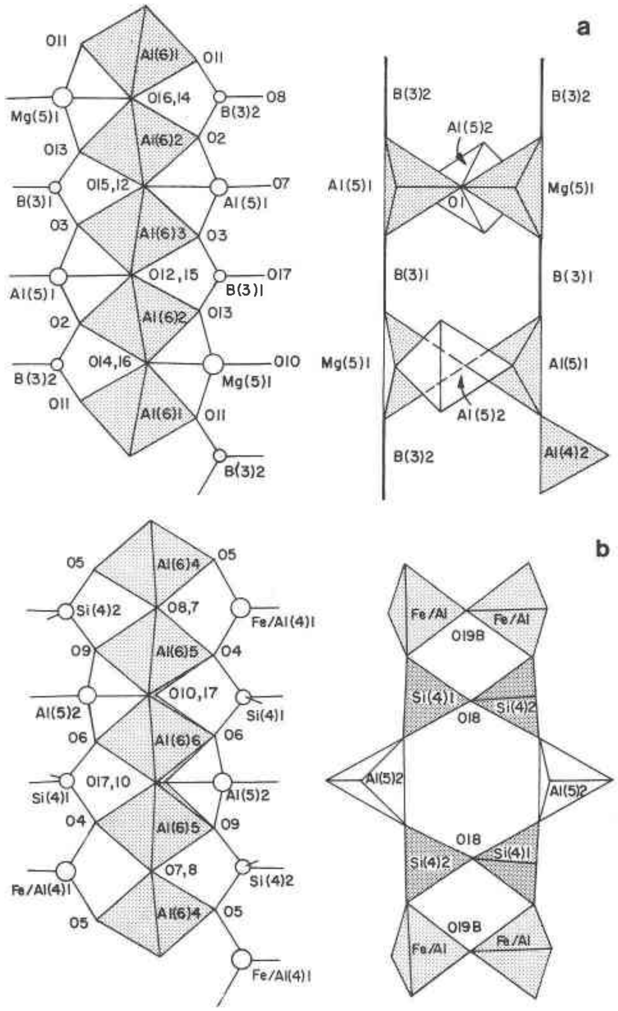

Fig. 2. Werdingite octahedral and polyhedral double chains, viewed normal to [001]. (**a**) Octahedral and polyhedral B-Mg-Al chains labeled A in Figure 1. (**b**) Octahedral and polyhedral Al/Fe-Si chains labeled B in Figure 1. Octahedral chains are viewed along the shared octahedral edges. Bridging chains are viewed normal to the plane containing the cations. BO_3 triangles appear as dark solid bars.

0.23. This corresponds to a B content per cell of 3.54, in excellent agreement with the chemical analysis.

The total Al content indicated by the refinement is 14.05 Al per cell, showing a small deficiency compared with the chemical analysis. We suggest that this is best described by a limited substitution in site Mg(5)1, in order to offset partially the excess Mg content of about 0.3 atoms which is implied by the refinement; regrettably we were unable to model this three-component site at Mg(5)1.

After the final refinement, the maximum residual electron density is located near Al(4)1 and no further improvement could be attained. The maximum and minimum residual densities are 1.72 and -1.80 eA^{-3}, respectively. Fractional atomic coordinates and temperature factors for werdingite are reported in Table 4, bond lengths and angles in Table 5, and a summary of atomic sites and occupancies in Table 6.

A bond-valence analysis (Brown, 1981) was applied as a test of the site allocations in the refinement. The results, presented in Table 7, show that most sites are balanced with approximately integral charges except for the multiply occupied sites Fe(4)1 and Mg(5)1 and the partially occupied sites B(3)2 and Al(4)2. The charge balance indicates that the cations occupying Fe(4)1 should be about 70% trivalent, which in turn suggests that the Fe allocated to this site is dominantly divalent. Mg(5)1, on the other hand, would be balanced if it were 30% occupied by trivalent cations, some of which are presumably Fe^{3+} cations.

Description of the structure

The unit cell of werdingite contains six octahedral aluminum sites, of which Al(6)1, Al(6)3, Al(6)4, and Al(6)6 lie on centers of symmetry, while Al(6)2 and Al(6)5 are on general positions. As shown in Figure 1, these Al polyhedra share edges to form two distinct chains running parallel to the **c**-axis, like those found in several other octahedral-chain aluminosilicates, such as sillimanite. Chain A (Fig. 2a) contains Al(6)1, Al(6)2 (linked by O14 and O16) and Al(6)3 (linked by O12 and O15). Octahedral chain B (Fig. 2b) contains Al(6)4, Al(6)5 (linked by (O7 and O8) and Al(6)6 (linked by O10 and O17). The **c**-axis repeat distance is equivalent to the height of four octahedral edges (11.406/4 = 2.851 Å). The octahedral Al-O distances are in the range 1.829(3)–1.979(3) Å, and the angles do not depart by more than 11° from the ideal values of 90 and 180° for the *cis*- and *trans*–O atoms respectively.

The two nonequivalent octahedral chains are linked by five-, four-, and three-coordinated cation sites (Fig. 2). The

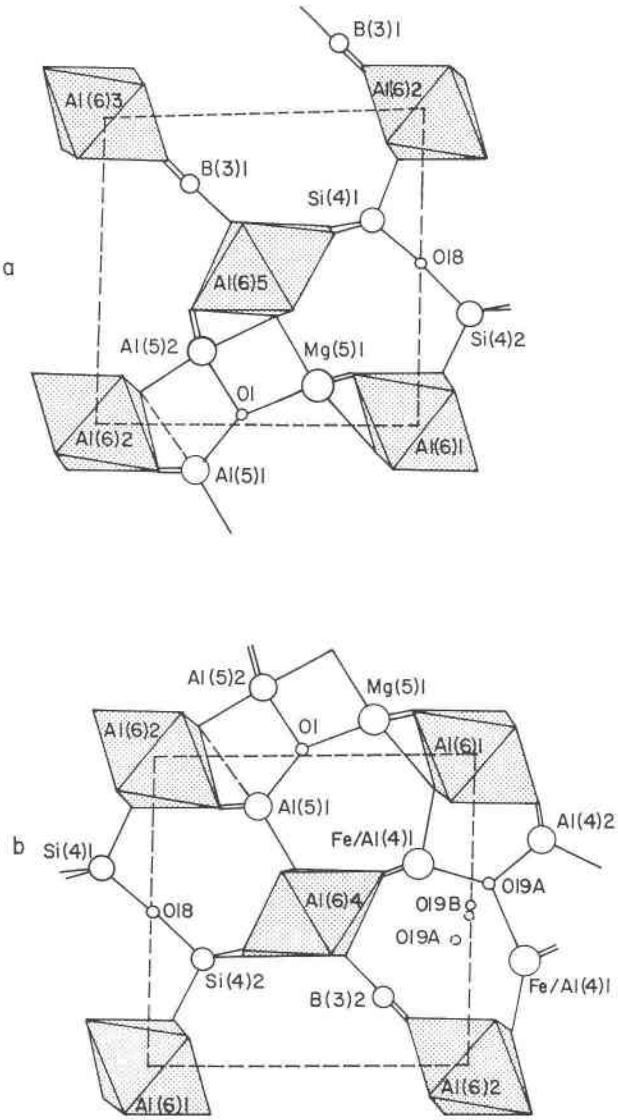

Fig. 3. Two mullite-like constitutent slabs of the werdingite unit cell, each bounded by Al octahedra in the corner chains, and containing four of the 16 bridging cation sites. (**a**) Al_2-[MgAlBSi]O_9 slab. (**b**) Al_2[Al(Al,Fe)BSi]$O_{9.5}$ slab. The long fifth bond to Al(5)1 is shown by a dashed line. In the adjacent slab to the right, B in B(3)2 has been replaced by Al in Al(4)2.

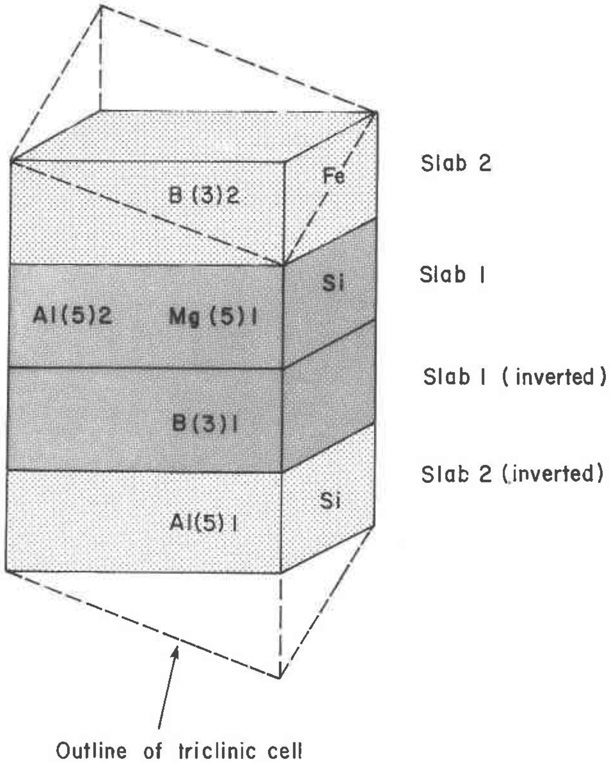

Fig. 4. Relationship of the triclinic unit cell (dashed outline) to the mullite-like slabs shown in Figure 3.

fivefold Al and Mg polyhedra may be described as irregular trigonal bipyramids. For the ideal trigonal bipyramid, one O-*X*-O angle is 180°, three are 120°, and the remaining six are 90°. Corresponding angles for Al(5)1, Al(5)2, and Mg(5)1 are in the ranges 168.4(2)–175.4(2)°, 109.2(2)–123.2(2)°, and 74.3(2)–111.1(2)°, respectively. In each polyhedron, the cation lies out of the plane of the equatorial triangle, so that one bond is distinctly longer than the remaining four. The shorter bond ranges in length from 1.742 to 1.824 Å for Al sites and from 1.901 to 1.973 Å for the Mg(5)1 site. For Al(5)2 and Mg(5)1 the long bonds are 11 and 12% greater in length, respectively, compared with 8% for the irregular five-coordinated Mg site in grandidierite. For Al(5)1, the fifth bond is 25% longer, and this site can be regarded alternatively as a tetrahedron.

The site Fe/Al(4)1 is coordinated by three O atoms yielding metal-oxygen bond lengths of approximately 1.826 Å. The distances to a fourth disordered O atom, lying on one of the O19A or O19B sites, range from 1.648 to 2.062 Å, and the angles between the disordered and the well-behaved O atoms range from 91.0 to 144.0°. Si-O tetrahedral distances fall in the range 1.617(2)–1.650(2) Å, and O-Si-O angles, in the range 106.8–111.7°, are close to the ideal value for a regular tetrahedron. The SiO_4 tetrahedra share an apex (O18) to form Si_2O_7 groups.

Both B sites are planar, almost equilateral triangles, with B-O distances of 1.360–1.427 Å.

Of the O sites, all but three are associated with the Al octahedral chains. The remainder, O1, O18, and O19A/B, constituting five O atoms per cell, link the polyhedra of bridging cations.

Discussion of the structure and comparison with grandidierite and sillimanite

The occurrence of Si_2O_7 groups indicates that werdingite could be described as a disilicate. To do so, however, obscures the close relationship with other octahedral-chain aluminosilicates such as the Al_2SiO_5 polymorphs. The arrangement of AlO_6 octahedral chains in werdingite is sim-

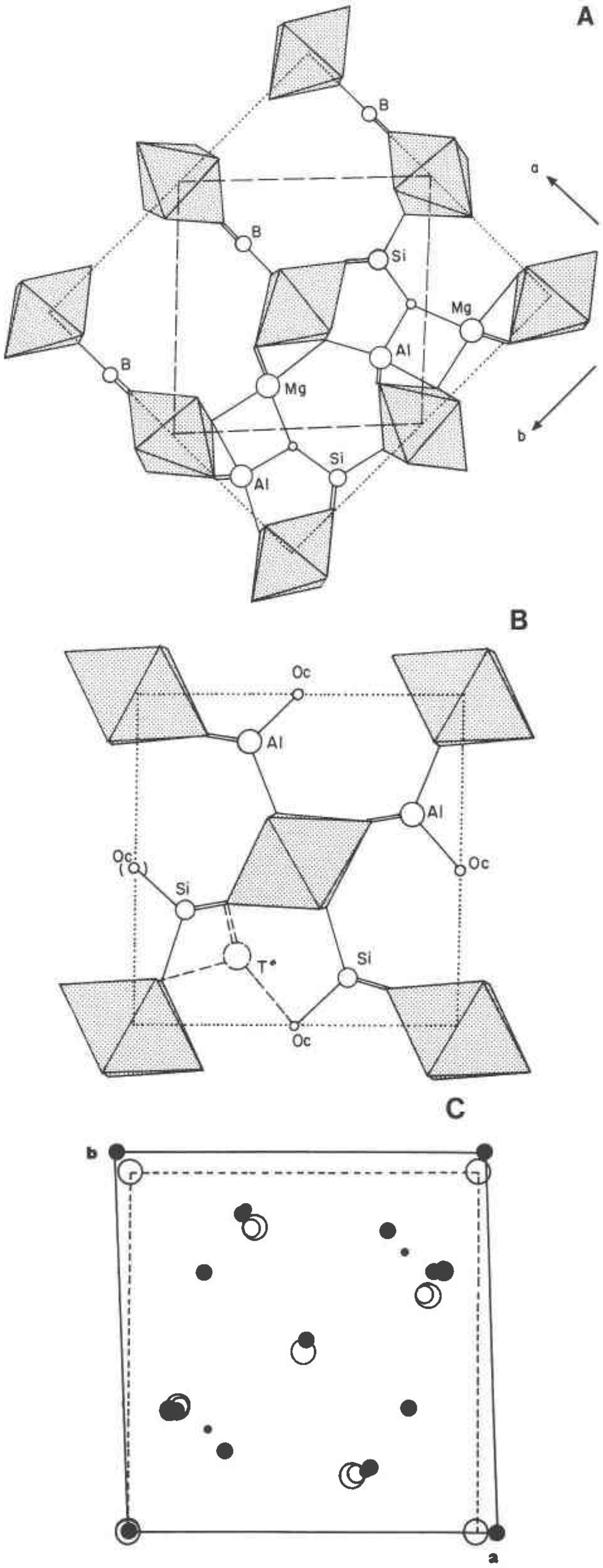

ilar to those in sillimanite and grandidierite, and the principal differences among these minerals involve the bridging cation sites. It is convenient to consider the werdingite structure as composed of two slabs, flattened normal to **c**, of approximate dimensions 7.5 × 7.6 × 2.8 Å (Fig. 3), which are stacked and inverted to make up the unit cell as shown in Figure 4. Each slab contains four of the 16 bridging cations, and the corners of the slab unit are defined by octahedral Al atoms in chain A. The slabs have dimensions similar to those of the unit cell of mullite. They are thus half the height of a sillimanite unit cell, and a representative unit of similar proportions can be formed from a quarter of a cell of the grandidierite structure (Fig. 5A).

A close structural relationship to the compositionally similar mineral grandidierite ($Al_2[AlMgBSi]O_9$) might be expected. Indeed, slab 1 of the werdingite structure (Fig. 3a) shows some similarities in local configuration. Two of the nonchain O sites are vacant, and the approximate formula of the slab is $Al_2[(Mg,Fe)AlBSi]O_9$. However, a comparison of Figures 3 and 5 shows that the superficial similarity indicated by the environment of B and the grouping of three bridging polyhedra does not extend to the longer-range configuration of bridging cations. In grandidierite, groupings of Al, Si, and Mg polyhedra alternate along **c** with large voids framed by BO_3 triangles, but the double chains of bridging polyhedra characteristic of werdingite (Fig. 2a) are not present. The composition of slab 2 is $Al_2[Al(Al,Fe)(B,Al)Si]0_{9.5}$, and here the bridging cations, except for B(3)2, are in near-tetrahedral coordination by anions.

The structure can alternatively be related to that of sillimanite, in which all the bridging cations are in tetrahedral coordination, with local rearrangements resulting from the removal of nonchain O atoms. A volume of sillimanite equivalent to that of the werdingite cell contains ${}^{[6]}Al_8[{}^{[4]}Al_8Si_8]O_{40}$, and thus three O atoms are missing from the werdingite structure. The double chains of alternating Al and Si tetrahedra parallel to the sillimanite **c** axis are replaced in the werdingite structure by the two types of polyhedral chains shown in Figure 2. The large voids produced by removing an O atom (equivalent to that in the O_c site of sillimanite) are framed by pairs of BO_3 triangles, or by displaced tetrahedral or five-coordinated sites, cross-linked to an adjacent polyhedral chain in a manner similar to that described for mullite in its

Fig. 5. Octahedral chain aluminosilicate structures related to werdingite. (**A**) View down [001] of lower half of the unit cell of grandidierite, after Stephenson and Moore (1968), reoriented for ← comparison with werdingite slab 1 (Fig. 2a). Grandidierite cell outlined by dotted line. Dashed lines mark a subunit equivalent in shape to one layer of cations within the werdingite cell. (**B**) View down [001] of lower half of sillimanite unit cell. Atomic displacements resulting from the substitution Al → Si + 0.5(O), as in mullite, shown by dashed lines. (**C**) Superimposed view down [001] of the cations of werdingite and sillimanite. Werdingite: cell outlined by solid line; cations are solid circles with radii Fe/Mg > Al = Al/Fe > Si > B. Sillimanite: cell outlined by dashed line; cations are open circles with radii Al > Si.

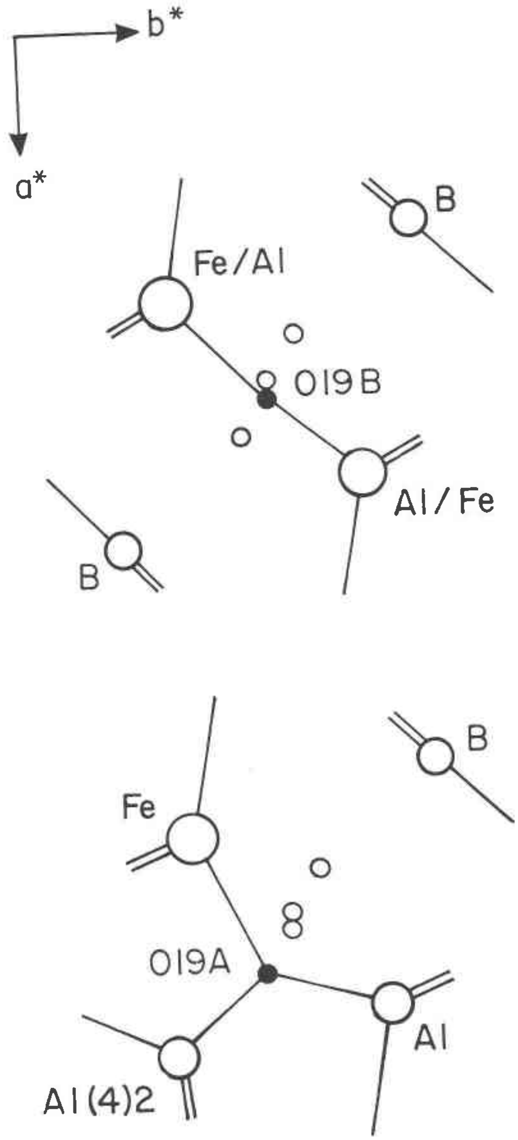

Fig. 6. Two possible configurations of cation and O site occupancy around the O19A and O19B sites in slab 2 of the werdingite structure, resulting from the substitution $^{[4]}Al \rightarrow {}^{[3]}B$, viewed down [001]. Two further configurations involving the upper O19A and O19B positions are symmetrically related to these.

relationship to sillimanite (Angel and Prewitt, 1986). Chain A shows a Si-Al ordering scheme opposite to that in sillimanite. The size difference between Si-Si and Al-Al pairs is accommodated by a zigzagging of the AlO_6 octahedral chains, which is in turn a consequence of the small B $^{[3]}B^{3+}$ cation pulling together alternate octahedral apices (Fig. 2a). The rotation of these Al octahedra is also responsible for bringing the larger bridging cations around O1 into five- rather than fourfold coordination.

The overall substitution relating werdingite to sillimanite can be written 2B + (Mg,Fe) = 2Si + Al + 1.5(O). This is identical to the substitution proposed for the accommodation of B in sillimanite with up to 0.42 wt% B_2O_3 by Grew and Hinthorne (1983) and Grew and Rossman (1985).

A notable feature of slab 2 of the werdingite structure is the positional disorder of O19, which is apparently distributed among four positions about the center of symmetry at 1/2,0,0, between the cation sites B(3)2, Al(4)2, Fe/Al(4)1, and their inverted equivalents in the adjacent cell. The idealized werdingite structure should have a single O atom at this special position. The chemical analysis and the refinement indicate that B(3)2 and Al(4)2 contain 77% B and 23% Al, respectively. Assuming that tetrahedral Al is bonded to O in O19A, the possible O configurations are likely to depend on the occupancy of neighboring B(3)2 and Al(4)2 sites, as shown in Figure 6. Furthermore, the four configurations should be equally represented when the Al occupancy is 33%, which is not greatly different from the case in the natural sample. Clearly only one of the two possible adjacent Al(4)2 sites can adopt tetrahedral coordination with a single O19, and this is likely to place an upper limit of one atom per formula unit on the Al = B substitution. It will be of interest to determine whether the O and cation disorder is random, or modulated. The effective size of the Fe(4)1 site and its distortion from tetrahedral symmetry are critically dependent on the position of the disordered O19, and the mean bond length ranges from 1.729 to 2.062 Å. The Fe cation is expected to prefer the largest configuration, in which Al occurs on one of the nearby Al(4)2 sites and is coordinated to an O atom in O19A. The refined occupancy of Al(4)2 implies that 0.23 of Fe(4)1 sites have long bonds to an O atom in O19A. The good match between this value and the refined Fe occupancy of Fe(4)1 (0.21) suggests a possible coupling between the Al → B and Fe → Al substitutions in these two sites.

Other structures related to werdingite

Sillimanite from certain high grade metamorphic rocks is known to contain up to 0.42% B_2O_3 (Grew and Hinthorne 1983). Sillimanite that is B rich also contains appreciable Mg, with an approximate cation ratio B:Mg of 2:1. Grew and Rossman (1985) showed that B substitution in the small Si site caused a change from regular tetrahedral to trigonal or near-trigonal coordination, and they suggested that there are local rearrangements of nearby cation sites into configurations like that in grandidierite, so that the overall substitution is 2B + Mg = 2Si + Al + 1.5(O).

Grandidierite, however, has a B:Mg ratio of 1:1. The relationship between werdingite and sillimanite structures suggests that these rearrangements, rather than resembling the structure of grandidierite, correspond to parts of the werdingite structure, and a possible model for the substitution is shown in Figure 7. The presence of B in threefold coordination causes the loss of an O atom from

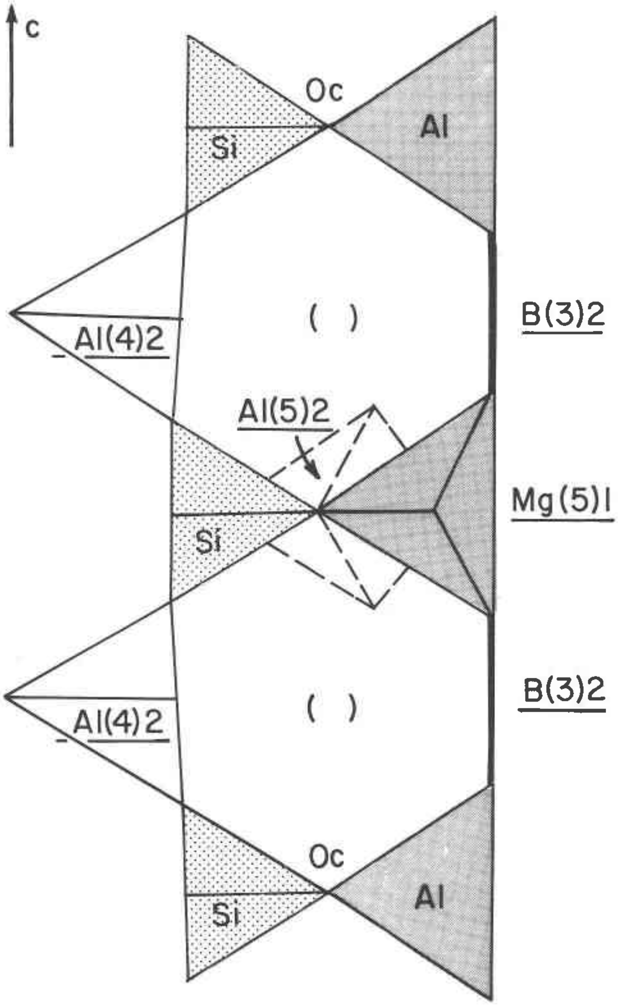

Fig. 7. A model for B substitution in sillimanite, in which an Al-Si tetrahedral double chain incorporates a werdingite-like section, with bridging O atoms O_c removed. B triangles are viewed edgewise. Parentheses mark the positions of vacant O sites, and underlined labels denote sites equivalent to those in werdingite (see Fig. 2a).

the O_c site, and the Al coordinated to this O_c site is presumed to be displaced into a mullite-like tetrahedral linkage to an adjacent polyhedral chain. To explain the incorporation of Mg, we propose that while the distortion caused by a single B substitution may not be sufficient to promote further rearrangement, the contraction resulting from two B atoms in alternate layers enlarges the intervening Al site so that occupation by the larger Mg cation is favored. The displacement toward the Mg site of an Al cation is accompanied by the loss of a third O atom from an adjacent polyhedral chain, and a small region resembling werdingite [but with Si taking the place of the near-tetrahedral Al(5)1] is produced (Fig. 7). An arrangement like this is presumed to be energetically more favorable than isolated or paired B → Si + 0.5(O) substitutions.

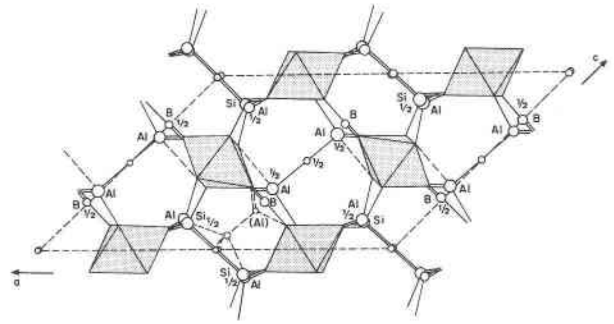

Fig. 8. A possible structure for $Al_8[Al_8(B,Al)_4Si_4]O_{38}$, the Mg-free B-rich mullite of Werding and Schreyer (1984), based on repetitions of werdingite slab 2.

Other schemes of local B and Mg substitution are possible, leading to werdingite-like domains of different size. As with the model shown in Figure 7, charge balance across the boundaries of these domains, from which integral numbers of O atoms are missing, is not easily achieved unless coupled with further replacements in the sillimanite structure, of which the most likely is the mullite substitution Al → Si + 0.5(O).

Sillimanite from the werdingite-bearing sample has 0.04 Mg atoms per formula unit of 20 O atoms, implying a B content of about double this value. This is comparable to the maximum B content of 0.08B per 20(O) recorded in sillimanite from kornerupine-bearing rocks by Grew and Hinthorne (1983). A limit to the substitution may be set by the necessary rearrangements to adjacent bridging chains. In particular, the werdingite structure has an entirely different tetrahedral Al-Si ordering scheme from that of sillimanite.

Further structural relationships are suggested by the products of synthesis studies in the system MgO-Al_2O_3-B_2O_3-SiO_2-H_2O by Werding and Schreyer (1984) and Werding (personal communication), which include new borosilicate phases with powder patterns resembling mullite. One of these is Al-rich, Mg-free B-rich mullite. A possible structure for this phase (Fig. 8) is based on repetitions of slab 2 of the werdingite structure, and has the overall ideal formula $^{[6]}Al_8[^{[5]}Al_4{}^{[4]}Al_4B_4Si_4]O_{38}$, with monoclinic symmetry ($C2/m$). In addition, if the substitution $^{[4]}Al \rightarrow {}^{[3]}B$ occurs, as in werdingite (Fig. 6), that phase can show variable B content. Further substitutions of the type B → Si + 0.5(O) in bridging polyhedral chain B lead eventually to a Si-free end-member $^{[6]}Al_8[^{[5]}Al_4{}^{[4]}Al_4B_{8-x}Al_x]O_{36}$, which may have orthorhombic symmetry if the polyhedral chains are equivalent. Scholze (1956) synthesized orthorhombic phases of composition $2Al_2O_3$:B_2O_3 and $9Al_2O_3$:$2B_2O_3$ at 1000 and 1100 °C respectively, with physical properties similar to those of mullite. The former corresponds to $x = 0$ in the above formula. The phase of composition $9Al_2O_3$:$2B_2O_3$ shows solid solution with mullite, and when its formula is normalized to 24 cations, it falls in the above solid solution range at $x = 3.64$, near the probable limit of this $^{[4]}Al \rightarrow {}^{[3]}B$ substitution at $x = 4$.

Conclusions

The structure determination of werdingite has revealed a B-bearing member of a family of AlO_6 octahedral chain structures based on sillimanite and mullite, and related by substitutions among the bridging cations, some of which involve the loss of nonchain O atoms (site O_c of sillimanite). The most important of these substitutions appear to be Al → Si + 0.5(O) (the mullite substitution) and B → Si + 0.5(O), which is apparently coupled with Mg → Al + 0.5(O) to derive the ideal magnesium werdingite structure, and which apparently also occurs in B-bearing sillimanite.

Internal substitutions within werdingite which may also occur in other members of the family include Fe → Mg in site Mg(5)1 and Fe → Al in site Fe/Al(4)1 and Al(4)2 → B(3)2. These last two substitutions may be coupled.

In werdingite the AlO_6 octahedral chains are linked by B triangles, whose small size causes a zigzag flexing of the chains. As a result there are different schemes of Al-Si ordering in the bridging polyhedra: werdingite, and possibly also B-rich mullite, shows Si-Si and Al-Al pairs in contrast to the alternating Si-Al tetrahedra in sillimanite. The same distortion of the octahedral chains causes some of the bridging cation sites to be five- rather than four-coordinated, but despite this there is no long-range similarity to the cation arrangements in grandidierite and andalusite.

Acknowledgments

We thank the University of Cape Town and the Foundation for Research and Development for financial support.

References cited

Angel, R. J., and Prewitt, C.T. (1986) Crystal structure of mullite: A re-examination of the average structure. American Mineralogist, 71, 1476–1482.

Brown, I.D. (1981) The bond-valence method: An empirical approach to chemical structure and bonding. In M. O'Keefe and A. Navrotsky, Eds., Structure and bonding in crystals II, p. 1–30. Academic Press, New York.

Cromer, D.T., and Liberman, D. (1970) Relativistic calculation of anomalous scattering factors for X-rays. Journal of Chemical Physics, 53, 1891–1898.

Cromer, D.T., and Mann, J.B. (1968) X-ray scattering factors computed from numerical Hartree-Fock wave functions. Acta Crystallographica, A24, 321–324.

Grew, E.S., and Hinthorne, J.R. (1983) Boron in sillimanite. Science, 221, 547–549.

Grew, E.S., and Rossman, G.R. (1985) Co-ordination of boron in sillimanite. Mineralogical Magazine, 49, 132–135.

Moore, J.M., Waters, D.J., and Niven, M.L. (1990) Werdingite, a new borosilicate mineral from the granulite facies of the western Namaqualand metamorphic complex, South Africa. American Mineralogist, 75, 415–420.

Nardelli, M. (1983) PARST: A system of computer routines for calculating molecular parameters from results of crystal structure analysis. Computing in Chemistry, 7, 95–98.

North, A.C.T., Phillips, D.C., and Matthews, S.F. (1968) A semi-empirical method of absorption correction. Acta Crystallographica, A24, 351–359.

Scholze, H. (1956) Uber Aluminiumborate. Zeitschrift für Anorganische und Allgemeine Chemie, 284, 272–277.

Sheldrick, G.M. (1978) SHELX76. In H. Schenk, R. Olthof-Hazekamp, H. van Koningsveld, and G.C. Bassi, Eds., Computing in crystallography, p. 34–42, Delft University Press, Holland.

Sheldrick, G.M. (1987) SHELXS-86. In G.M. Sheldrick, C. Kruger, and R. Goddard, Eds., Crystallographic computing, p. 175–178, Oxford University Press, England.

Stephenson, D.A., and Moore, P.B. (1968) The crystal structure of grandidierite $(Mg,Fe)Al_3SiBO_9$. Acta Crystallographica, B24, 1518–1522.

Werding, G., and Schreyer, W. (1984) Alkali-free toumaline in the system MgO-Al_2O_3-B_2O_3-SiO_2-H_2O. Geochimica et Cosmochimica Acta, 48, 1331–1344.

Manuscript received March 16, 1990
Manuscript accepted November 9, 1990